Critical state and magnetization loss in multifilamentary superconducting wire solved through the commercial finite element code ANSYS

2010 Supercond. Sci. Technol. 23 115004

(http://iopscience.iop.org/0953-2048/23/11/115004)

Supercond. Sci. Technol. **23** (2010) 115004 (14pp) doi:10.1088/0953-2048/23/11/115004

Critical state and magnetization loss in multifilamentary superconducting wire solved through the commercial finite element code ANSYS

S Farinon[1], P Fabbricatore[1] and F Gömöry[2]

[1] INFN-Sezione di Genova, Via Dodecaneso, 33, 16146 Genova, Italy
[2] Institute of Electrical Engineering, Slovak Academy of Sciences, Dúbravská cesta 9, 842 39 Bratislava, Slovakia

E-mail: stefania.farinon@ge.infn.it

Received 29 June 2010, in final form 2 September 2010
Published 30 September 2010
Online at stacks.iop.org/SUST/23/115004

Abstract
The commercially available finite element code ANSYS has been adapted to solve the critical state of single strips and multifilamentary tapes. We studied a special algorithm which approaches the critical state by an iterative adjustment of the material resistivity. Then, we proved its validity by comparing the results obtained for a thin strip to the Brand theory for the transport current and magnetization cases. Also, the challenging calculation of the magnetization loss of a real multifilamentary BSCCO tape showed the usefulness of our method. Finally, we developed several methods to enhance the speed of convergence, making the proposed process quite competitive in the existing survey of ac losses simulations.

(Some figures in this article are in colour only in the electronic version)

1. Introduction

HTS are serious candidates for applications in electrical energy transportation and devices. Consequently, one of the main tasks in the conductor design is to minimize the ac dissipation due to the cyclic variations of transport current and the electrical and magnetic fields. In this framework, the possibility to predict the losses by numerical calculations is of fundamental importance for optimizing the industrial development of wires. The usual approach to simulate the losses consist in including a power law $E = \rho(J/J_C)^n$ in the Maxwell equation set. This procedure often converges very slowly, because typically $n \gg 10$, motivating the search for a simpler, faster converging process. Due to its robustness, we decided to use the finite element code ANSYS™ [1], even if at first glance it appears an inappropriate tool in not allowing the definition of any resistivity dependence of the type $\rho = \rho(J)$.

2. General description of the critical state algorithm

The basic idea of this work was to develop a simple and fast method allowing the evaluation of the ac losses of a single superconducting wire of arbitrary cross section (or a distribution of wires), with either an oscillating transport current or applied magnetic field. The Bean critical state model [2] coupled to finite element analysis seemed a viable approach to solve the above mentioned problem. The critical state was first introduced by Bean and describes a superconducting material through its critical current density, J_C, which is an upper limit to the current density which can flow in the superconductor itself. It can be demonstrated [3, 4] that this corresponds to a flux penetration from the wire edges, such that the magnetic field is null where the current density is less than J_C, and it can assume values different from zero only when $|J| = J_C$. The main consequence is that the critical state model does not depend on time (or frequency of the applied load) and the ac losses are uniquely determined by the field profiles at the peak value of the applied load (either current or external magnetic field). This means that one single calculation at the peak applied load contains the information of the whole cycle, thus saving a large amount of calculation time and effort. We decided to try solving the field profiles with a method based on the widely diffused finite

element code ANSYS. The main drawback of this choice is that there is no straightforward way to implement the critical state in the finite element analysis, as the program does not allow a relation to be defined between the current density and the resistivity of the superconducting material, as required to perform the numerical calculation. Nevertheless, there is a way to iteratively converge [5] to the correct resistivity distribution by following a very simple algorithm. First, the transient electromagnetic problem is solved for a constant resistivity ρ equal in all $i = 1, \ldots, M$ regions into which the wire cross section is divided. Next, the resistivity of each i-element is iteratively changed according to

$$\rho_i^{k+1} = \max\left\{\rho_i^k \frac{|J_i^k|}{J_C}, \rho_0\right\} \tag{1}$$

until

$$\frac{|\rho_i^{k+1} - \rho_i^k|}{\rho_i^k} < \varepsilon \tag{2}$$

where k is the cycle index, ε the convergence parameter and ρ_0 the minimum meaningful value of the resistivity. This procedure corresponds to finding a resistivity distribution among the elements which determines the current density to be everywhere less than or equal to the critical current density, as prescribed by the critical state model.

Since this process does not descend from any physical equation or theory, it is necessary to assess its validity by comparing its results, in terms of field and current density profiles and ac losses, to specific cases for which there exist analytical solutions. This will prove that the proposed algorithm logically behaves as the critical state does, justifying its application to more general cases. Therefore, we tested our algorithm in two cases, in the thin strip with transport current and in a perpendicular magnetic field, for which analytical solutions were found by Brandt in [4]. As stated, the algorithm has been implemented in the finite element software ANSYS, using the ANSYS parametric design language (APDL).

3. Solution of the thin strip in transport current

Let us consider a thin strip, $2a$ in width and d in thickness ($d \ll a$), having J_C (A m^{-2}) as the critical current density and carrying a transport current $I_a = I_a(t)$. It can be demonstrated [4] that the current density and field profiles inside the strip when increasing the current from 0 to I_a are:

$$J(x) = \begin{cases} \dfrac{2J_C}{\pi} \arctan\sqrt{\dfrac{a^2-b^2}{b^2-x^2}} & |x| < b \\ J_C & b < |x| < a \end{cases} \tag{3}$$

$$B(x) = \begin{cases} 0 & |x| < b \\ \dfrac{B_C x}{|x|} \operatorname{arctanh}\sqrt{\dfrac{x^2-b^2}{a^2-b^2}} & b < |x| < a \end{cases} \tag{4}$$

where

$$B_C = \mu_0 J_C d/\pi, \qquad I_a = 2J_C d\sqrt{a^2-b^2}, \qquad b = a\sqrt{1 - I_a^2/I_{\max}^2} \tag{5}$$

and $I_{\max} = 2adJ_C$ is the maximum total current occurring at full penetration $b = 0$. The energy per unit length dissipated in a cycle (J m^{-1}) is found to be [4]

$$P = \mu_0 I_{\max}^2/\pi f(I_a/I_{\max}) \qquad f(z) = (1-z)\ln(1-z) + (1+z)\ln(1+z) - z^2. \tag{6}$$

Combining the Maxwell equation $\int_{\partial S} \mathbf{E}\cdot \mathrm{d}\ell = \partial\Phi_{B,S}/\partial t$ with Ohm's law $\mathbf{E} = \rho\mathbf{J}$, and using the current density and the field profiles respectively as in (3) and (4), the resistivity can be determined as

$$\rho(x) = \begin{cases} 0 & |x| < b \\ \dfrac{2\mu_0 d}{\pi \Delta t} g(x) & b < |x| < a \end{cases} \tag{7}$$

where

$$g(x) = |x| \operatorname{atanh}\sqrt{\frac{x^2-b^2}{a^2-b^2}} - a \operatorname{atanh}\left(\frac{a}{|x|}\sqrt{\frac{x^2-b^2}{a^2-b^2}}\right) + \sqrt{a^2-b^2}\ln\left(\frac{\sqrt{x^2-b^2}+|x|}{b}\right) \tag{8}$$

and Δt is the time needed to reach the current I_a.

As an example, let us model, using the finite element code ANSYS, a thin strip with $a = 200$ μm, $d = 2$ μm (aspect ratio $\alpha = d/a = 0.01$), $J_C = 1 \times 10^7$ A m^{-2}, so that $I_{\max} = 2adJ_C = 8$ mA. Due to the symmetry of the problem it is possible to model only 1/4 of the strip, using for instance 200 elements, each 1 μm^2 in section. The two parameters governing the algorithm can be set to $\rho_0 = 1 \times 10^{-16}$ Ω m and $\varepsilon = 10^{-4}$. The value of ρ_0 has been chosen in such a way that a further reduction would affect no more the final result within the desired accuracy of the convergence parameter ε.

Comparisons of the current density, magnetic field and resistivity profiles inside the strip, as calculated by the finite element analysis and by the corresponding analytical expressions, are shown in figures 1–3, respectively. It is clear that the agreement is very good, confirming the validity of the critical state algorithm used to obtain these results. In its implementation, the analytical expression (7) for the resistivity has been replaced by

$$\rho(x) = \begin{cases} \rho_0 & |x| < b \\ \dfrac{2\mu_0 d}{\pi \Delta t} g(x) + \rho_0 & b < |x| < a \end{cases} \tag{9}$$

to be consistent with the ANSYS calculations.

The last point to assess the validity of the critical state algorithm consists in the evaluation of the ac losses, comparing them to (6). Taking advantage of the fact that there always exist a 'kernel' (using the Norris terminology), that is a 'fiber' carrying no current at any time (except perhaps during an infinitesimal period at peak current flow) [3], the ac losses per unit length (J m^{-1}) can be written as the integral over time of the Poynting vector [6]

$$P(I_a) = 2\int_{-I_a}^{I_a} \mathbf{E}\cdot\mathbf{J}\,\mathrm{d}t = 4\int J(x,y)\Phi(x,y)\,\mathrm{d}S \tag{10}$$

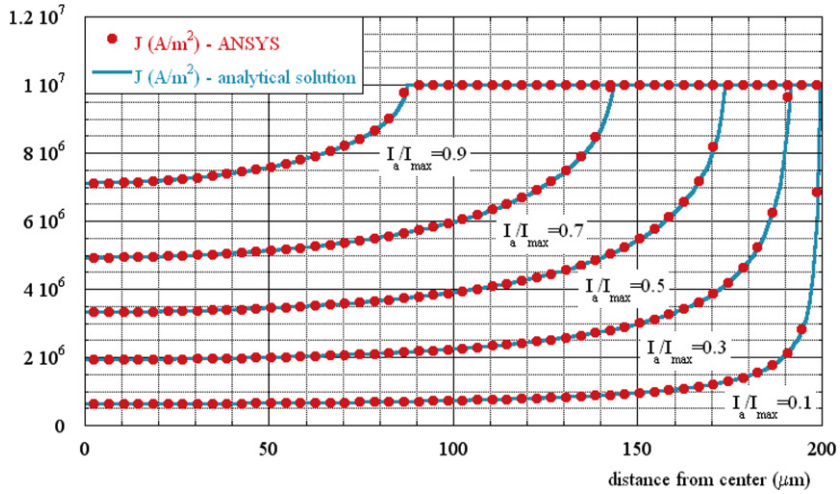

Figure 1. Current density profiles of a thin strip ($a = 200\ \mu$m, $d = 2\ \mu$m, $J_C = 1 \times 10^7$ A m^{-2}) in transport current for various values of the ratio I_a/I_{max} as calculated by ANSYS (red dots) and using the analytical expression (3) (blue lines).

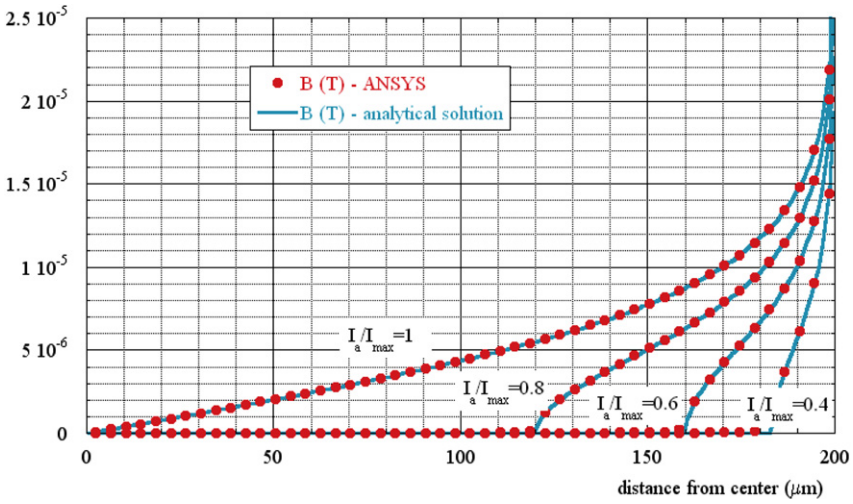

Figure 2. Magnetic field profiles of a thin strip ($a = 200\ \mu$m, $d = 2\ \mu$m, $J_C = 1 \times 10^7$ A m^{-2}) in transport current for various values of the ratio I_a/I_{max} as calculated by ANSYS (red dots) and using the analytical expression (4) (blue lines).

where $\Phi(x, y) = \int \mathbf{B} \cdot \mathbf{n}\, d\ell$ is the flux calculated with respect to the kernel, ℓ is a line connecting (x, y) to the kernel, $\mathbf{B}$ is the local magnetic field and $\mathbf{n}$ is the unit vector normal to this line. Thus, $\mathbf{B} \cdot \mathbf{n}$ is the length of the projection of the total magnetic field (transverse + perpendicular) onto the normal vector. Moreover, since $J = J_C$ when $B \neq 0$ and $B = 0$ when $J < J_C$, it is possible to write [7]

$$P(I_a) = 4J_C \sum_{\text{all elements with } J=J_C} \left(\int \mathbf{B} \cdot \mathbf{n}\, d\ell \right) \Delta_S \qquad (11)$$

where Δ_S is the cross-sectional area of each element. In a symmetric problem, the kernel can be easily identified with the origin of the axes.

Figure 4 shows the ac losses per unit length normalized to $\mu_0 I_{max}^2/\pi$ as function of the ratio $z = I_a/I_{max}$, as calculated by ANSYS for different strip aspect ratios $\alpha = d/a$ and compared to the analytical expression $f(z) = (1 - z)\ln(1 - z) + (1 + z)\ln(1+z) - z^2$. The agreement is quite good, especially for the thinnest strip ($\alpha = 0.01$) with $I_a/I_{max} > 0.5$. There is a clear effect of the finite thickness of the strip when compared to a theory which is valid for an infinitely thin structure. This effect enters the calculation through (11), stating that each element contributes to the losses proportionally to the component of the magnetic field along the normal to the line connecting the center of each element to the axes origin, $B_n(x, y)$, as sketched in figure 5.

In contrast, in the theory only the field perpendicular to the strip width contributes to the losses. Secondly, the error in the integration is larger for small values of I_a/I_{max}, as the integration is performed on a smaller number of elements, i.e. all the elements which carry J_C. If $N(I_a/I_{max})$ is the number of 'excited' elements for a given value of the applied current, we have $N(0.1) = 1$, $N(0.2) = 4$, $N(0.3) = 9$, $N(0.4) = 17$. This error was found to be less than 5% and can be overcome very easily, in case we need very accurate ac losses when $I_a/I_{max} \leqslant 0.4$: a finer mesh size in the region

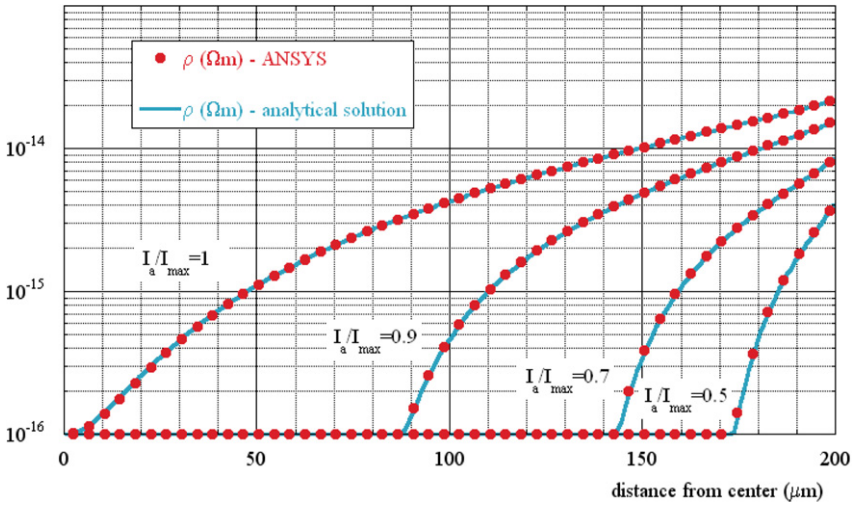

Figure 3. Resistivity profiles of a thin strip ($a = 200\ \mu$m, $d = 2\ \mu$m, $J_C = 1 \times 10^7$ A m^{-2}) in transport current for various values of the ratio I_a/I_{max} as calculated by ANSYS (red dots) and using the analytical expression (7) (blue lines). In all cases $\Delta t = 0.01$ s.

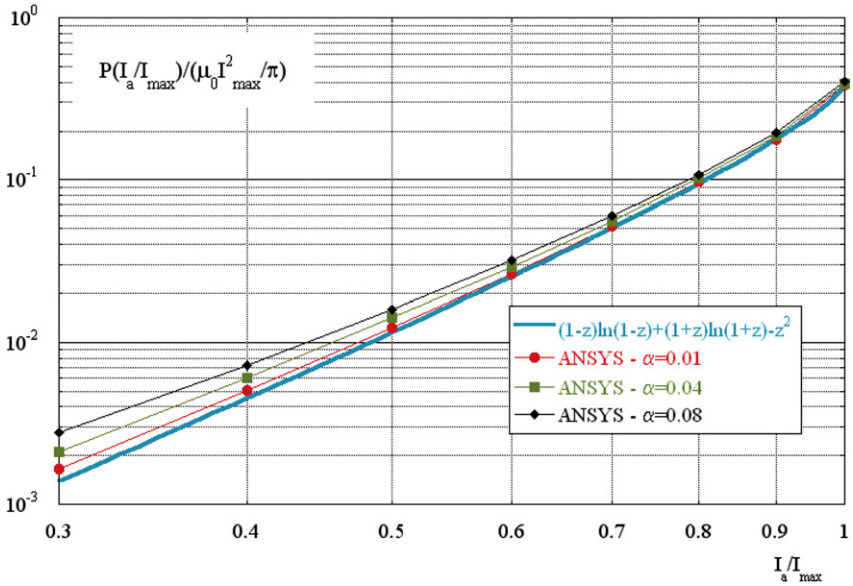

Figure 4. Ac losses per unit length normalized to $\mu_0 I^2_{max}/\pi$ as function of the ratio $z = I_a/I_{max}$ as calculated by ANSYS for different strip aspect ratios $\alpha = d/a$ (colored shapes) and using the analytical expression (6) (blue line).

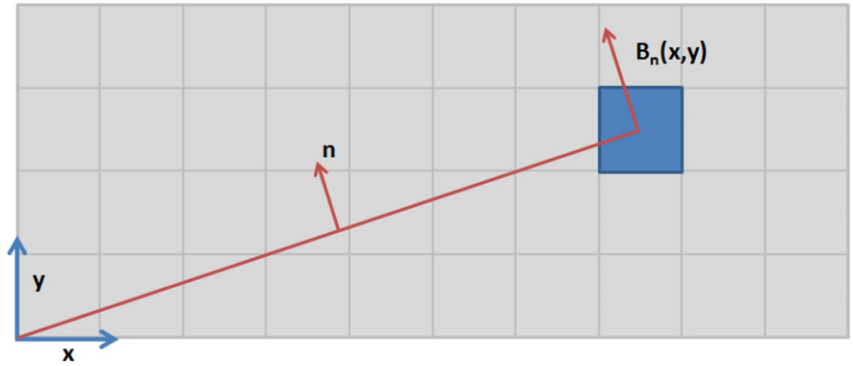

Figure 5. Sketch of the single strip finite element mesh showing the contribution of the i-element to the losses as proportional to the component of the magnetic field along the normal to the line connecting the center of each element to the axes origin.

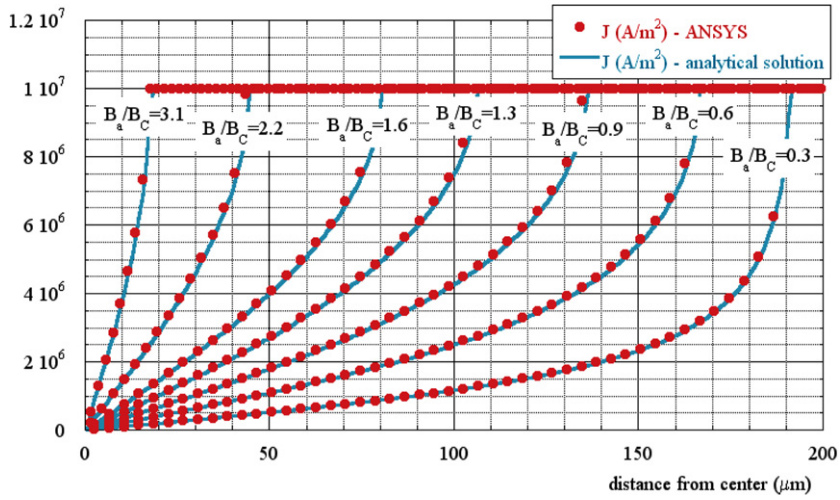

Figure 6. Current density profiles of a thin strip ($a = 200\ \mu$m, $d = 2\ \mu$m, $J_C = 1 \times 10^7$ A m^{-2}) in a perpendicular magnetic field, for various values of the ratio B_a/B_C, as calculated by ANSYS (red dots) and using the analytical expression (12) (blue lines).

where the penetration occurs is enough to get any required accuracy.

4. Solution of the thin strip in a perpendicular applied field

Let us consider the same thin strip, $2a$ in width and d in thickness ($d \ll a$), having J_C (A m^{-2}) as the critical current density and exposed to a magnetic field $B_a = B_a(t)$ perpendicular to its width. It can be demonstrated [4] that the current density and field profiles inside the strip while increasing the external magnetic field from 0 to B_a are:

$$J(x) = \begin{cases} \dfrac{2J_C}{\pi} \arctan\left(\dfrac{cx}{\sqrt{b^2 - x^2}}\right) & |x| < b \\ \dfrac{J_C x}{|x|} & b < |x| < a \end{cases} \tag{12}$$

$$B(x) = \begin{cases} 0 & |x| < b \\ B_C \operatorname{arctanh}\left(\dfrac{\sqrt{b^2 - x^2}}{c|x|}\right) & b < |x| < a \end{cases} \tag{13}$$

where

$$B_C = \mu_0 J_C d/\pi, \qquad b = a/\cosh(B_a/B_C), \qquad c = \sqrt{a^2 - b^2}/a = \tanh(B_a/B_C). \tag{14}$$

Defining $I_C = 2ad\,J_C$, the energy per unit length dissipated in a cycle (J m^{-1}) is found to be

$$P = \mu_0 I_C^2/\pi\, F(B_a/B_C) \qquad F(z) = 2\ln\cosh z - z\tanh z. \tag{15}$$

Combining the Maxwell equation $\int_{\partial S} \mathbf{E}\cdot \mathrm{d}\ell = \partial\Phi_{B,S}/\partial t$ with the Ohm's law $\mathbf{E} = \rho\mathbf{J}$, and using the current density and the field profiles respectively as in (12) and (13), the resistivity can be determined as

$$\rho(x) = \begin{cases} 0 & |x| < b \\ \dfrac{2\mu_0 d}{\pi\,\Delta t} G(x) & b < |x| < a \end{cases} \tag{16}$$

where

$$G(x) = |x|\operatorname{atanh}\sqrt{\frac{x^2 - b^2}{c|x|}} - a\operatorname{atanh}\sqrt{\frac{x^2 - b^2}{ac}} \tag{17}$$

and Δt is the time needed to reach the magnetic field B_a.

Let us model again, using the finite element code ANSYS, a thin strip with $a = 200\ \mu$m, $d = 2\ \mu$m (aspect ratio $\alpha = d/a = 0.01$), $J_C = 1 \times 10^7$ A m^{-2}, so that $I_C = 2ad\,J_C = 8$ mA. Due to the symmetry of the problem it is possible to model only 1/4 of the strip, using for instance 200 elements, each 1 μm^2 in section. As before, the two parameters governing the algorithm can be set to $\rho_0 = 1 \times 10^{-16}\ \Omega$ m and $\varepsilon = 10^{-4}$.

A comparison of the current density, magnetic field and resistivity profiles inside the strip, as calculated by the finite element analysis and by the corresponding analytical expressions, is shown in figures 6–8, respectively. It is clear that the agreement is very good, confirming the validity of the critical state algorithm for simulating also the case of an external applied field. Similarly to the calculation for the transport case, the analytical expression (16) for the resistivity has been replaced by

$$\rho(x) = \begin{cases} \rho_0 & |x| < b \\ \dfrac{2\mu_0 d}{\pi\,\Delta t} G(x) + \rho_0 & b < |x| < a \end{cases} \tag{18}$$

to be consistent with the ANSYS calculations.

The ac losses in an applied magnetic field can be calculated using (11) or through the magnetization curves. In

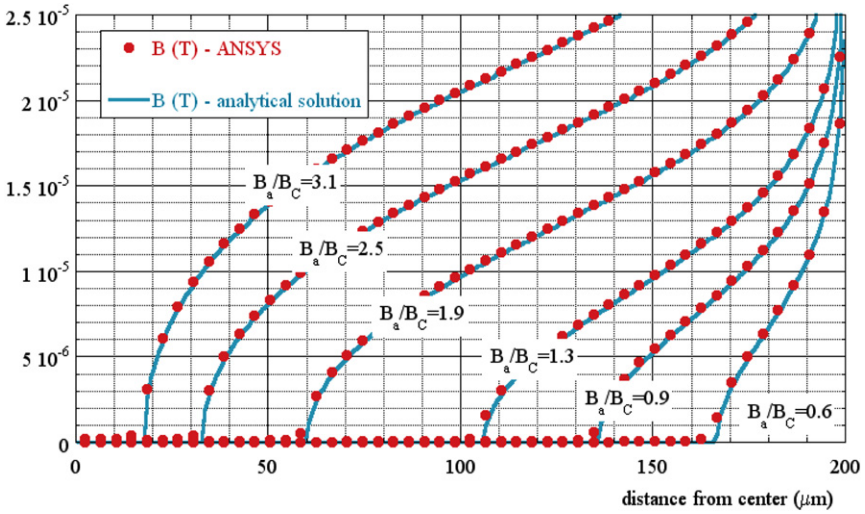

Figure 7. Magnetic field profiles of a thin strip ($a = 200\ \mu$m, $d = 2\ \mu$m, $J_C = 1 \times 10^7$ A m^{-2}) in a perpendicular magnetic field, for various values of the ratio B_a/B_C, as calculated by ANSYS (red dots) and using the analytical expression (13) (blue lines).

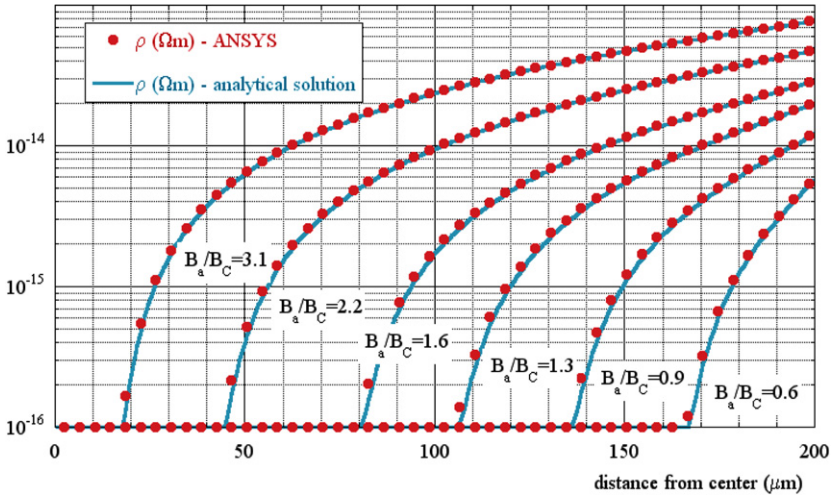

Figure 8. Resistivity profiles of a thin strip ($a = 200\ \mu$m, $d = 2\ \mu$m, $J_C = 1 \times 10^7$ A m^{-2}) in a perpendicular magnetic field, for various values of the ratio B_a/B_C, as calculated by ANSYS (red dots) and using the analytical expression (18) (blue lines). In all cases $\Delta t = 0.01$ s.

fact, in a perpendicular applied field, the ac losses per unit length can be calculated as:

$$P(B_a) = \oint m(B_a)\,\mathrm{d}B_a \tag{19}$$

where $m(B)$ is the total magnetic moment per unit length in the direction of the applied field:

$$m(B_a) = -\int x \times J(B_a)\,\mathrm{d}S. \tag{20}$$

Following [8], one can demonstrate that, within the Bean critical state model, the full hysteresis loop of the magnetic moment m in a cycled applied field with amplitude B_0 is completely determined by the virgin magnetization curve $m(B_a)$:

$$\begin{aligned} m_{\downarrow}(B_a, B_0) &= m(B_0) - 2m\left(\frac{B_a - B_0}{2}\right) \\ m_{\uparrow}(B_a, B_0) &= -m(B_0) + 2m\left(\frac{B_a + B_0}{2}\right). \end{aligned} \tag{21}$$

It should be noted that, whilst in the first method the losses at a certain applied field B_a only depend on the field distribution inside the strip at that applied field, using the magnetization loops the losses at B_a depend on the history of the magnetic moment while increasing the external field from 0 to B_a. The main consequence is that to determine the losses at a given applied field we need one single calculation using (11) and at least ten calculations using the magnetization loops (the minimum number is that which allows the determination of the integral of the loop with the required degree of accuracy).

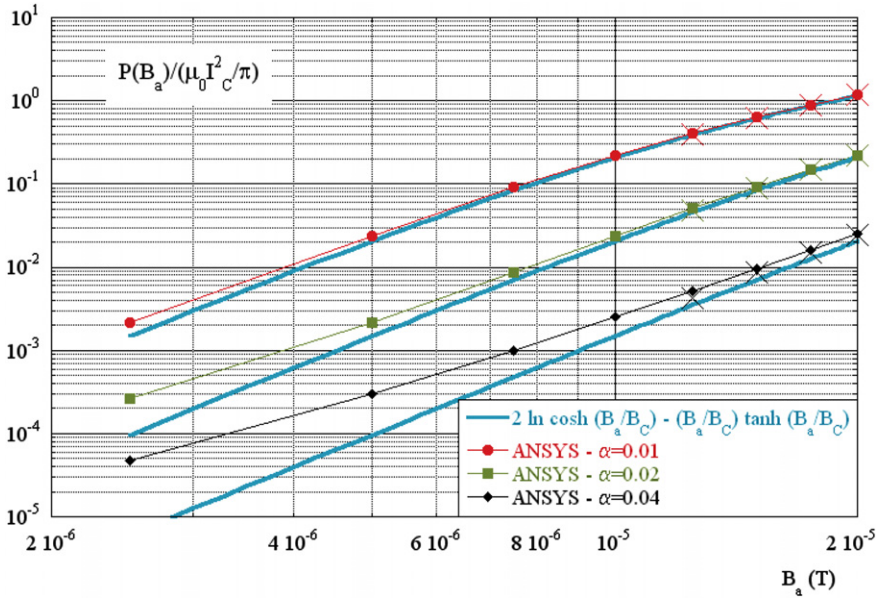

Figure 9. Ac losses per unit length normalized to $\mu_0 I_C^2/\pi$ as a function of B_a as calculated by ANSYS for different strip aspect ratios $\alpha = d/a$ through the Poynting vector (full symbols) or the magnetization loops (crosses) and using the analytical expression (15) (blue lines).

Figure 9 shows the ac losses per unit length normalized to $\mu_0 I_C^2/\pi$ as a function of B_a as calculated by ANSYS for different strip aspect ratios $\alpha = d/a$ using both methods and compared to the analytical expression $F(z) = 2\ln\cosh z - z\tanh z$.

Due to the strong demagnetizing factor of a strip in a perpendicular field, the agreement is quite good only for the thinnest strip ($\alpha = 0.01$). In order to analyze thoroughly this effect and, more generally, the behavior of a superconducting sample in an external applied magnetic field, it is very useful to introduce the so called ac susceptibility, a quantity that can be calculated through our analytical and numerical models and possibly compared to existing measurements. The basic concepts of ac susceptibility can be found in [9]. Here we recall that ac susceptibility can be expressed as $\chi = \chi_0(\chi' - \mathrm{i}\chi'')$, where we have introduced the magnetization M as the total magnetic moment per unit volume:

$$\chi = \mu_0 \frac{\mathrm{d}M}{\mathrm{d}B_a}, \qquad \chi_0 = \mu_0 \left.\frac{\mathrm{d}M}{\mathrm{d}B_a}\right|_{B_a \ll B_C}. \tag{22}$$

The importance of ac susceptibility lies in the fact that its imaginary component can be directly linked to the ac losses per unit volume q in an external applied magnetic field B_a through the expression [10]:

$$q = \pi \chi_0 \chi'' \frac{B_a}{\mu_0}. \tag{23}$$

Since χ'' ranges from 0 to 0.3–0.4 as function of the applied field for whatever sample, it is clear that ac losses are strongly dominated by χ_0, the so called external susceptibility. Particularly in the case of the strip in a perpendicular magnetic field, the expression for χ_0 reduces to

$$\chi_0 = \left.\frac{\mu_0}{2ad}\frac{\mathrm{d}m(B_a)}{\mathrm{d}B_a}\right|_{B_a=0} = \frac{\mu_0}{2ad}\frac{\mathrm{d}}{\mathrm{d}B_a}[J_C a^2 d \tanh(B_a/B_C)]|_{B_a=0} = \frac{\pi}{2}\frac{a}{d} \tag{24}$$

and the line tangent to $m(B_a)$ for $B_a \sim 0$ is $m(B_a) = (\pi a^2/\mu_0)B_a$. This is confirmed by the finite element analysis, as shown in figure 11, which then gives the correct evaluation of χ_0. This explains why, for the strip in a perpendicular field, the agreement shown in figure 9 is quite good only for the thinnest strip ($\alpha = 0.01$). In fact, ac losses being inversely proportional to the aspect ratio of the strip, the comparison between theory and finite element analysis is meaningful only for very small aspect ratios.

5. Ac losses of a BSCCO multifilamentary wire

In order to check the method we developed, we next considered the multifilamentary BSSCO tape we have analyzed several times in the past [11–15]. It is a Bi-2223/Ag composite tape with 19 superconducting filaments embedded in a silver matrix, manufactured by the Institute of Electrical Engineering of the Slovak Academy of Sciences [16, 17]. The cross section of its filamentary region, together with the corresponding finite element model at full penetration, is shown in figure 10. Measured ac susceptibility data have been used to determine the losses per cycle in the volume unit of the tape, according to (23). Thus, we can compare either the measured χ'' with χ'' derived from calculated ac losses and χ_0 or calculated ac losses with losses derived from the measured χ'' and calculated χ_0. In both cases, we need to determine χ_0.

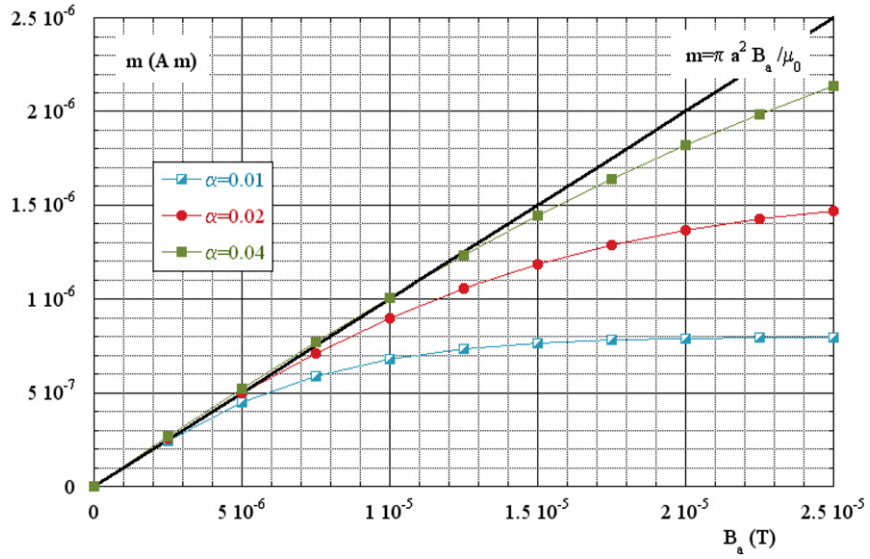

Figure 10. Total magnetic moment per unit length as function of the applied field for different strip aspect ratios $\alpha = d/a$.

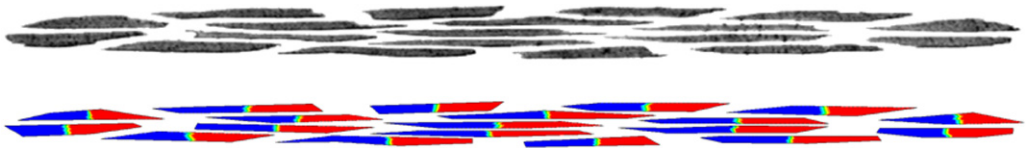

Figure 11. Cross section of the BSCCO tape filamentary region, together with the corresponding finite element model at full penetration (blue represents $-J_C$, red $+J_C$).

5.1. Determination of χ_0

Before proceeding with the determination of χ_0, more precise information is necessary. In fact, χ_0 can be determined in two ways. First, taking advantage of the fact that in the pure Meissner state (perfect shielding) the magnetization of a superconductor is uniform, χ_0 can be expressed in term of the energy variation per unit length ΔW when a sample of magnetic permeability $\mu_r \ll 1$ is introduced in a medium of magnetic permeability μ_0 immersed in a uniform magnetic field B_a [11–13]:

$$\chi_0 = \frac{\Delta W}{\frac{B_a^2}{2\mu_0} A_{\text{sample}}}. \tag{25}$$

The other method, involving the simulation of the critical state for an applied field much less than the critical field, determines χ_0 as

$$\chi_0 = \mu_0 \frac{\mathrm{d}M}{\mathrm{d}B_a}\bigg|_{B_a \ll B_C} = \frac{\mu_0}{A_{\text{sample}}} \frac{\mathrm{d}m(B_a)}{\mathrm{d}B_a}\bigg|_{B_a \ll B_C} \tag{26}$$

where $m(B_a)$ is the total magnetic moment per unit length. In both cases, there is a normalization with respect to the cross section of the sample. If the sample is mono-core, like an isolated strip, the meaning of A_{sample} is clear, it coincides with the cross-sectional area of the sample itself. If the sample is more complicated, like a composite tape, its meaning is less obvious [18]. Let us consider for instance a cylindrical sample immersed in a magnetic field normal to its axis. It can be very easily calculated that $\chi_0 = 2$ [19]. If now consider a hollow cylinder, χ_0 must still to be two, because for a very small value of the applied field the central part of the sample is inactive, so there is no way to discriminate between the two samples. For the same reason, also the energy variation to introduce the sample in a uniform magnetic field is the same. As a consequence, to obtain the same value for χ_0 in both cases we need to divide the energy variation by the same section, the superconducting section in the full cylinder case, the shielded section in the hollow cylinder case.

In the case of the 19 filament tape, the determination of the shielded section is not straightforward. A way to estimate it is to define the shielded section as the area of the filaments plus the internal 'shielded' regions, where there is no path for the magnetic flux lines.

In figure 12 the flux lines in the filamentary area of the BSCCO tape in the case of perfect shielding and the corresponding shielded cross section obtained by comparison are shown. The shielded cross section is found to be around 33% larger than the superconducting section. The two values of χ_0 calculated using (25) are:

$$\chi_{0\,\text{S/C}} = 36, \qquad \chi_{0\,\text{shield}} = 27. \tag{27}$$

In order to cross check this result, we can also calculate χ_0 through (26). In this case we need to determine the total momentum per unit length for very small values of the applied field. In figure 13 the momentum per unit length

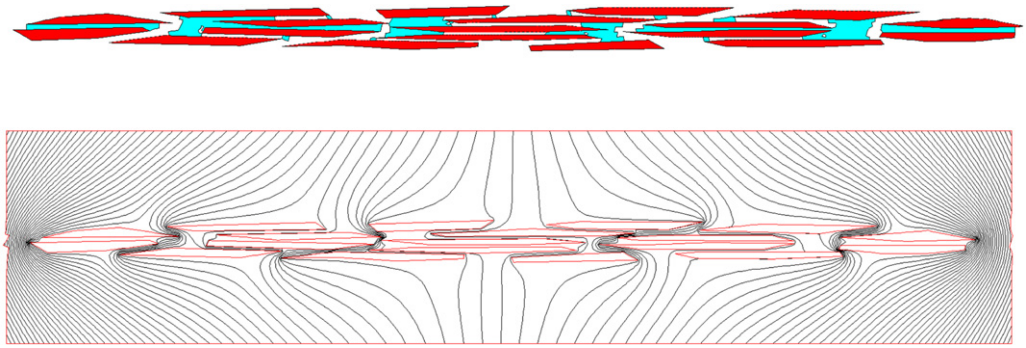

Figure 12. Flux lines in the filamentary area of the BSCCO tape in the case of perfect shielding (bottom) and the corresponding shielded cross section (top), filament regions in red and 'shielded' internal regions in light blue.

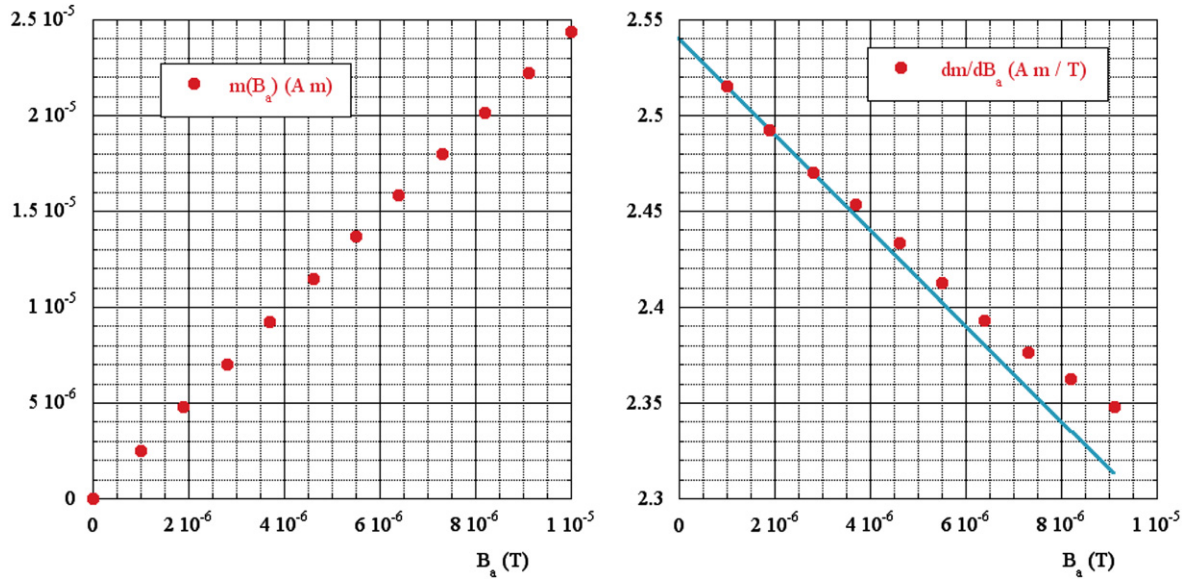

Figure 13. Total momentum per unit length (left) and its derivative with respect to the applied field (right) for the BSCCO tape.

and its derivative with respect to the applied field are shown. Extrapolating for $B_a \to 0$, $\mathrm{d}m/\mathrm{d}B_a \to 2.54$. Using this result to determine χ_0:

$$\chi_{0\ \mathrm{S/C}} = 35, \qquad \chi_{0\ \mathrm{shield}} = 26 \tag{28}$$

which agrees well with the values of χ_0 previously calculated through the energy variation in the Meissner state.

5.2. Ac susceptibility and ac losses

We can now make a comparison between our calculation and measurements in terms of ac susceptibility and ac losses per unit length, linked together by

$$P = \pi \chi_0 \chi'' \frac{B_a}{\mu_0} A_{\mathrm{S/C}}. \tag{29}$$

In this case there is no doubt about $A_{\mathrm{S/C}}$, which has to be the area of the superconducting filaments, which is where dissipation really occurs. The measurement was performed at 80 K, 35 Hz and a superimposed dc field of 100 G, this last in order to depress the dependence of J_{C} on the applied field.

In the finite element model we have one single parameter which can be used to optimize the fit, that is J_{C}. Moreover we can also adjust the value of χ_0 in order to get the measured amplification. The best agreement, shown in figures 14 and 15, is found for $J_{\mathrm{C}} = 0.385 \times 10^8$ A m^{-2} and $\chi_0 = 26$, confirming that χ_0 normalized to the shielded volume is the correct amplification factor of the ac losses. It is interesting to note that the value of the χ'' peak does not depend on J_{C}: by varying J_{C} the χ'' peak occurs at different values of the applied field but always assumes the same value, which is only related to the geometry of the sample.

In order to have an idea of what happens inside the tape, we can plot the current density averaged over the whole superconducting cross section divided by J_{C} as a function of the applied field, as shown in figure 16. This ratio, in fact, represents the percentage of the filament area which is penetrated by J_{C}, and obviously has to tend to 100% for the full penetrated configuration shown in figure 11. The χ'' peak corresponds roughly to a 70% penetration of the current density.

Some technical details on speeding up the calculation process are given in the appendix.

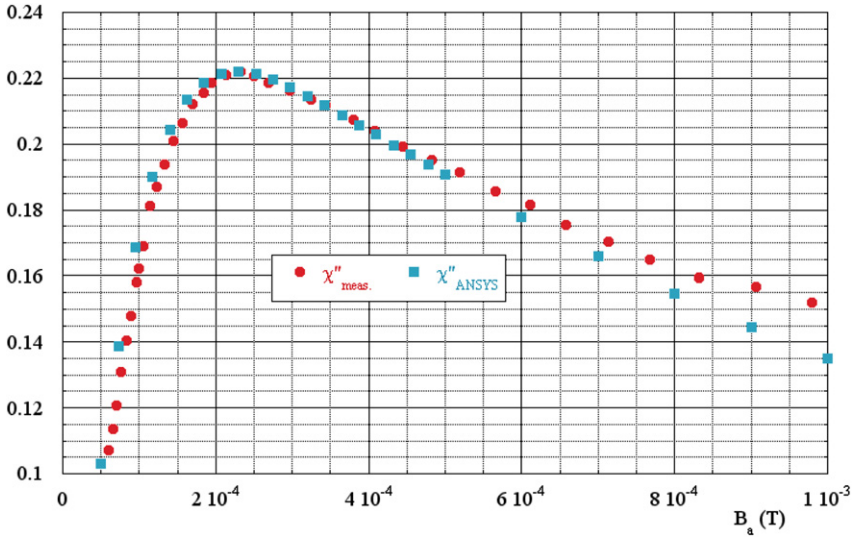

Figure 14. χ'' as measured and as calculated by ANSYS using $J_C = 0.385 \times 10^8$ A m^{-2} and $\chi_0 = 26$ as fitting parameters.

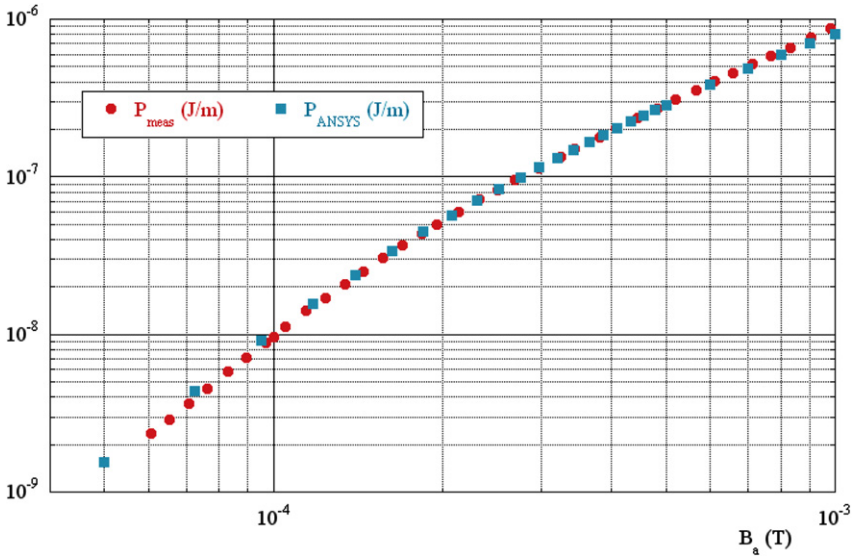

Figure 15. Dissipated energy per unit length as calculated by ANSYS and as obtained by χ'' measurement using $J_C = 0.385 \times 10^8$ A m^{-2} and $\chi_0 = 26$ as fitting parameters.

6. Generalization of the method

The method for simulating the critical state we proposed has been validated through the comparison with conductor geometries for which either analytical solutions exist or experimental data are available. Nevertheless, it can be applied with good results to any conductor shape and even to any distribution of conductors. As an example, we show in figure 17 typical flux profiles induced by a transverse field in an isolated wire and in three wires lined up in the polar and in the equatorial direction, as obtained through our numerical analysis. These are classical configurations which can be qualitatively compared for instance with [20] (page 170). A quantitative analysis cannot be carried out because analytical formula do not exist in these cases, we only verified that in the isolated wire case the calculated value of χ_0 is two, as predicted by theory.

7. Conclusions

We have proved that the proposed method, based on the commercial finite element code ANSYS, is qualified to calculate the distribution of electrical current in a superconducting wire according to the Bean critical state model, in both transport current and an applied perpendicular magnetic field. Its main advantage consists in the use of a powerful professional finite element code allowing its application to real wire geometries. In calculating the ac loss

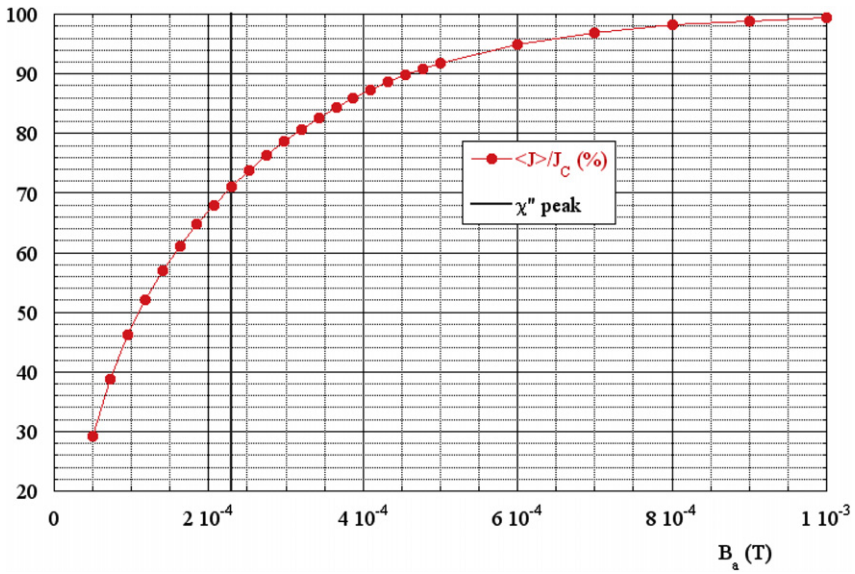

Figure 16. Average current density over the whole cross section divided by the critical current density as a function of the applied field.

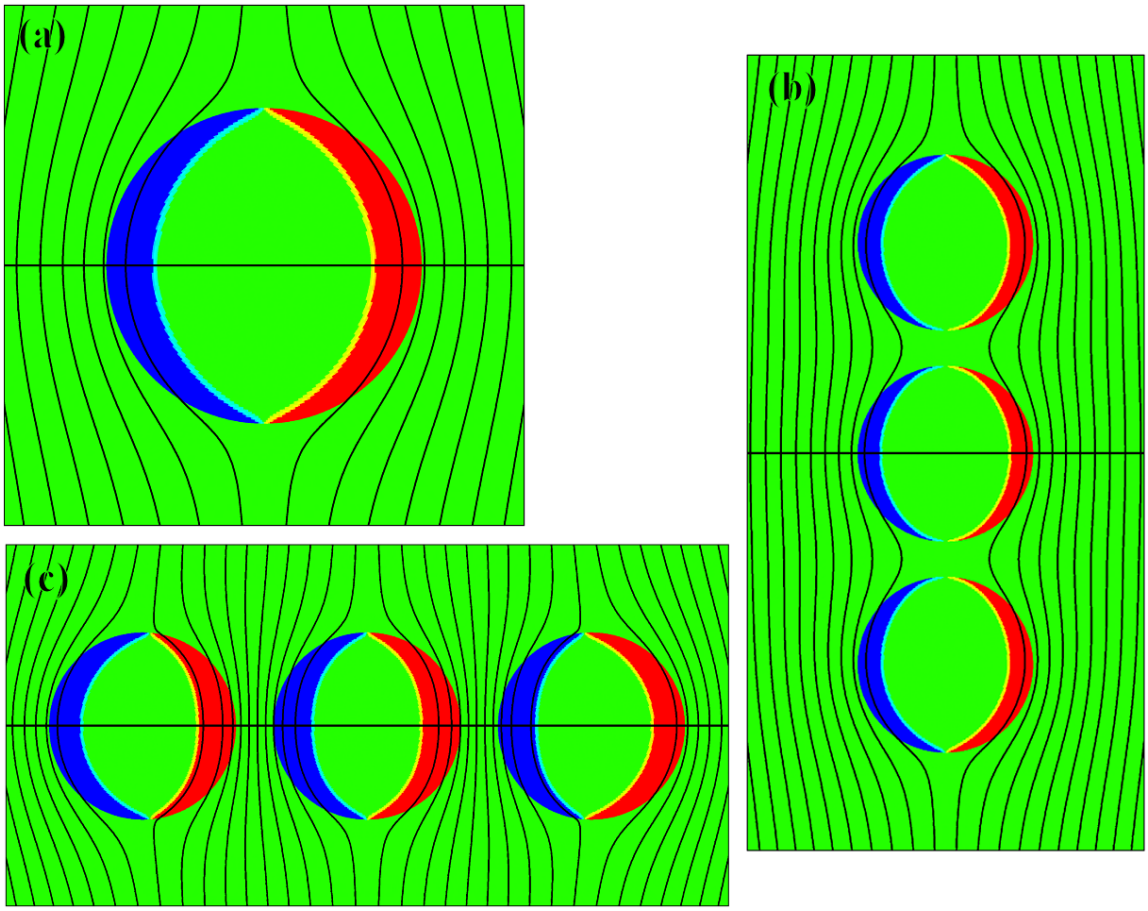

Figure 17. Magnetic field profiles and screening current densities (blue or dark grey represents $-J_C$, red or grey $+J_C$), as calculated through the proposed method, induced by a transverse field in three configurations: (a) isolated cylindrical wire, (b) three wires lined up in the polar direction, (c) three wires lined up in the equatorial direction.

we used the fact that the virgin solution, raising the applied load from an unexcited configuration, completely determines any possible critical state. The applicability of our method has been demonstrated to the calculation of magnetization loss in Bi-2223/Ag wire with a rather complicated shape of filaments after a heavy deformation process. In this calculation we used

J_C and χ_0 as fitting parameters. We also found that there are wide margins of enhancement of the convergence speed, in terms of the total number of iterations needed to get the final result with the required accuracy.

Acknowledgment

The authors wish to thank Dr Andrea Chincarini for his fruitful suggestions on the algorithm convergence.

Appendix. A method to speed up the algorithm convergence

Due to the peculiarity of the algorithm described in section 2, we can define the time needed for convergence independently of the CPU performance, as the number of iterations needed to obtain a specified accuracy. The total CPU time can be then obtained roughly by multiplying the number of iterations by the time needed to carry out one single iteration (which is not far from being a constant). This is because each single iteration starts over again, without the need to save and retrieve bigger and bigger files, which would slow down the calculation speed.

In order to compare different procedures, it is necessary to define a benchmark, representative of the procedure itself. We decided to take consider a strip ($a = 200\ \mu$m, $d = 2\ \mu$m, $J_C = 10^7$ A m^{-2}, meshed with 200 elements) in transport current when the applied current I_a is raised from 0 to I_{max} in one single shot, without taking advantage of the resistivity distribution obtained at previously converged values of I_a, which would consistently reduce the number of iterations of each step. Moreover, we can set $\rho_0 = 1 \times 10^{-16}\ \Omega$ m and $\varepsilon = 10^{-4}$. With a mesh of ~113 000 nodes, each iteration takes around 17 s on an HP Workstation with a Core 2 Quad Q9400 Processor and 8 GB RAM.

First of all, we notice that the convergence rule (1) is not uniquely identified. It can be replaced by

$$\rho_i^{k+1} = \max\{\rho_i^k f(x_i^k), \rho_0\} \tag{30}$$

where $x_i^k = |J_i^k|/J_C$ and $f(x)$ is a monotonically increasing function such that $f(0) = 0$ and $f(1) = 1$. $f(x) = x$ is the benchmark case. As a first attempt, we can try several functions which are continuous with continuous first derivative. The real acting part of this function is for $x \gtrsim 1$: in fact, starting from a uniformly distributed resistivity set to ρ_0, the first cycle will result in a very high current density at the extremities of the strip and around zero elsewhere. The next cycle will then assign a larger resistivity to the extremities, in such a way as to reduce J to J_C, and leave the resistivity unchanged elsewhere. The new current density distribution will present a new peak, much higher that J_C, in the elements adjacent to the previously modified ones. Again, the resistivity of this new group of elements is increased to get $J < J_C$. Iterating, one can understand that the behavior of $f(x)$ which determines the rate of convergence is when $x = J/J_C$ is over or around one. Table A.1 summarizes some of the tested functions together with the number of iterations needed for convergence. There are two important remarks: first there is a clear dependence of the number of iterations for convergence, N, on the first derivative of $f(x)$ calculated at $x = 1$, as it can be seen in figure 17, very well fitted by the power law $N = 467/[f'(1)]^{0.77}$. Second, for $f'(1) = 2$ there is an abrupt change, the system starts to oscillate and no longer converges. This characteristic does not depend on any of the model parameters (J_C, ρ_0, ε, mesh size, applied loads, ...) and it is a typical behavior of a feedback system, i.e. a system where the output signal is sent back to the input iteratively. However, there is a quite important margin of improvement: the number of iterations at $f'(1) = 1.95$ is 60% of that at $f'(1) = 1$, the benchmark function.

Table A.1. Number of iterations needed for the convergence of the benchmark case for different functions in normal and accelerated conditions.

Function $f(x)$	$f'(1)$	Number of iterations normal	Number of iterations accelerated
$f(x) = x$	1	469	230
$f(x) = \sqrt{x}$	0.5	799	474
$f(x) = x^2$	2	Does not converge	Does not converge
$f(x) = \ln_2(1 + x)$	0.721	600	305
$f(x) = 2^x - 1$	1.386	360	162
$f(x) = 0.2x^2 + 0.8x$	1.2	404	187
$f(x) = 0.6x^2 + 0.4x$	1.6	326	150
$f(x) = 0.8x^2 + 0.2x$	1.8	299	234

A way to further improve the rate of convergence is to take advantage of the numerous algorithms which have been developed in the past to accelerate a sequence. In fact, for each i-element, we can interpret the iterative algorithm $\rho_i^{k+1} = \rho_i^k f(x_i^k)$ as a mere converging numerical sequence, so we can try to apply existing tools of convergence enhancement. In particular, we selected one of the most simple procedures, Aitken's delta-squared process, first introduce by Aitken in 1926 [21].

Given a sequence y^k, $k \in \mathbb{N}$, one associates with this sequence the new sequence

$$Ay^k = \frac{y^{k+2}y^k - (y^{k+1})^2}{y^{k+2} - 2y^{k+1} + y^k}. \tag{31}$$

It can be demonstrated that the transformation Ay^k can be used to improve the rate of convergence of a slowly converging sequence because, empirically, it eliminates the largest part of the absolute error.

To understand the effectiveness of this acceleration process, we concentrate on the behavior of the most external element ($x = 200\ \mu$m) of our benchmark strip. In figure A.2 the resistivity of that element as a function of the number of iterations using the function $f(x) = 1$ in normal and accelerated conditions is shown. It is evident that the resistivity of the accelerated sequence is already not far from its converged value after around 50 iterations, and it converges with the required accuracy ($\varepsilon = 10^{-4}$) after 230 iterations, around half the number in normal conditions.

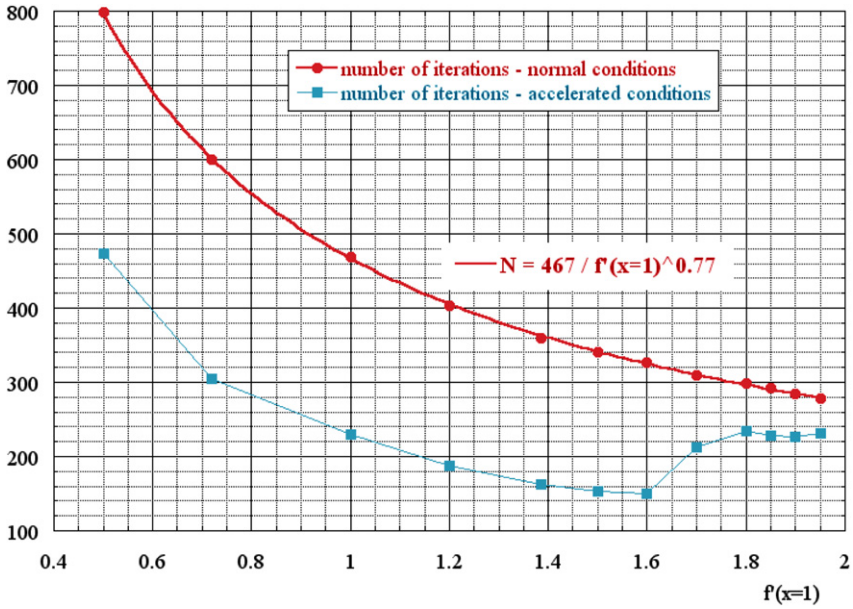

Figure A.1. Number of iterations to get convergence of the benchmark case as a function of $f'(x = 1)$ for the different tested functions in normal and accelerated conditions.

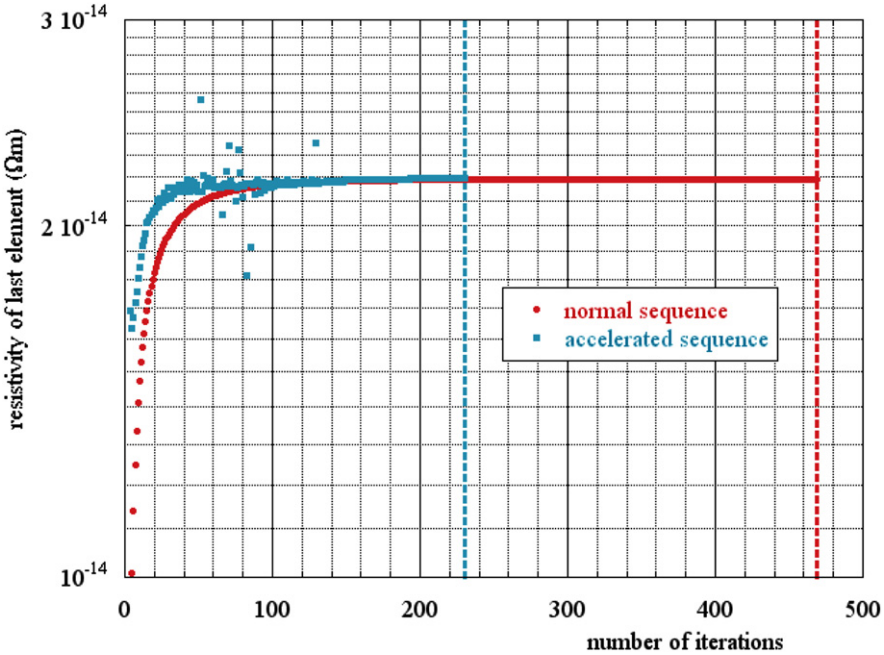

Figure A.2. Resistivity of the last element ($x = 200\ \mu$m) as function of the number of iterations for $f(x) = x$ in normal (red dots) and accelerated conditions (blue squares).

Figure A.1 shows the number of iterations to get convergence as function of $f'(1)$ for the different tested functions in normal and accelerated conditions: in accelerated condition its behavior is more irregular than in normal conditions, nevertheless it still gets oscillating for $f'(1) \geqslant 2$ and improves the convergence for any $f'(1) < 2$. In particular, a minimum can be identified for $f'(1) \approx 1.6$, leading to the best enhancement: the number of iterations using a function with $f'(1) = 1.6$ and accelerating the sequence is the 34% of that obtained using the standard function $f(x) = x$ without acceleration.

References

[1] ANSYS Multiphysics, Release 11 ANSYS Inc. www.ansys.com
[2] Bean C P 1970 *J. Appl. Phys.* **41** 2482
[3] Norris W T 1970 *J. Phys. D: Appl. Phys.* **3** 489
[4] Brandt E H and Indebom M 1993 *Phys. Rev.* B **48** 893

[5] Gu C and Han Z 2005 *IEEE Trans. Appl. Supercond.* **15** 2859
[6] Carr W J 1983 *AC Loss and Macroscopic Theory of Superconductors* (London: Gordon and Breach)
[7] Daumling M 1998 *Supercond. Sci. Technol.* **11** 590
[8] Brandt E H 1998 *Phys. Rev.* B **58** 6523
[9] Gömöry F 1997 *Supercond. Sci. Technol.* **10** 523
[10] Clem J R and Sanchez A 1994 *Phys. Rev.* B **50** 9355
[11] Fabbricatore P, Farinon S and Innocenti S 2000 *Phys. Rev.* B **61** 6413
[12] Fabbricatore P, Farinon S, Gömöry F and Innocenti 2000 *Supercond. Sci. Technol.* **13** 1327
[13] Fabbricatore P, Farinon S, Gömöry F and Seiler E 2001 *IEEE Trans. Appl. Supercond.* **11** 2776
[14] Gömöry F, Ŝouc J, Fabbricatore P, Farinon S, Stryček F, Kováč P and Hušek I 2002 *Physica* C **371** 229
[15] Gömöry F *et al* 2004 *Supercond. Sci. Technol.* **17** S150
[16] Kováč P, Hušek I and Kopera L 1997 *Supercond. Sci. Technol.* **10** 982
[17] Kováč P, Hušek I, Rosova A and Pachla W 1999 *Physica* C **312** 179
[18] Fabbricatore P, Farinon S, Incardone S, Gambardella U, Saggese A and Volpini G 2009 *J. Appl. Phys.* **106** 083905
[19] Goldfarb R B 1986 *Cryogenics* **26** 621
[20] Wilson M N 1983 *Superconducting Magnets* (Oxford: Oxford Science Publications)
[21] Aitken A 1926 *Proc. R. Soc. Edinburgh* **46** 289